RSC Applied Polymers

ROYAL SOCIETY OF CHEMISTRY

PAPER

View Article Online
View Journal | View Issue

Cite this: *RSC Appl. Polym.*, 2025, **3**, 1193

A roll-to-roll chitosan finishing strategy for elastane recovery†

Eleanor C. Grosvenor, ‡[a] Malachi Cohen,‡[a] Caterina Czibula,[a,b] Emma M. Sellin,[a] Kayla T. Ghezzi,[c] Natalie C. Fisher,[a] Jana B. Schaubeder, [b] Sara E. Branovsky, [a] Gabrielle N. Wood,[a,d] Jeffrey J. Richards [c] and Cécile A. C. Chazot *[a]

Received 11th July 2025,
Accepted 20th July 2025

DOI: 10.1039/d5lp00213c

rsc.li/rscapplpolym

Elastane fibers, renowned for their balanced strength, elasticity, and comfort, are a prevalent component in blended fabrics. However, their strong adhesion within core-spun yarns and resistance to chemical dissolution pose significant challenges for separation and recycling. The lack of a universal single-solvent strategy across blend types limits the scalability of selective dissolution recycling. Here, we propose an alternative approach using a dissolvable chitosan (CS) finishing layer applied to elastane fibers, which can be selectively removed at end-of-life to enable separation from sheath fibers. We implemented a continuous dip-coating process and demonstrated its feasibility at pilot scale using a roll-to-roll setup. By tuning solution viscosity, we achieved uniform, conformal coatings on neat elastane. A 4 wt% CS solution in 0.5 N HCl yielded a 5–10 μm-thick coating that forms strong non-covalent interactions with the elastane core without compromising the elastic modulus or energy dissipation under cyclic strain. The CS layer can be redissolved under mild acidic conditions, preserving the chemical integrity of the recovered elastane. This proof-of-concept highlights CS dip-coating as a promising finishing strategy for scalable elastane recovery from diverse fiber blends *via* selective dissolution.

Introduction

Clothing is an important means of self-expression with nuanced social, cultural, and even political implications. Rapid trend cycles and population growth drive the demand for new styles, which led textile manufacturers to produce 124 million tons of garments in 2024. Future garment production is projected to reach 160 million tons by 2030.[1,2] This growth generates substantial waste, with roughly 18 million tons of material discarded by the garment industry alone in 2020.[3,4] Synthetic fibers comprise 57% of this waste,[1] making them a major contributor. Due to the difficulty in separating synthetic fibers in scalable recycling streams, over 70% of clothing fibers end up in landfills or incinerated, with less than 1% recycled into new garments.[5,6]

Elastane, also known as spandex or LYCRA® fiber, is ubiquitous in the textile industry. Elastane fibers contain at least 85% polyurethane–polyurea, a linear block copolymer with alternating rigid and flexible segments.[7,8] The flexible segments allow elastane to be reversibly stretched by up to 600%,[9,10] and the rigid segments participate in hydrogen bonding, providing strength to the fiber.[9] The balance between elasticity and tenacity (fiber tensile strength) of elastane yarns can be modulated simply by changing the denier (mass in grams per 9000 meters of fiber).[11] As a result, stretch fabrics containing even small amounts of elastane (~1–5%) are comfortable without sacrificing tear strength,[11–13] underscoring its popularity in sportswear and casual wear. For most applications, elastane is blended with other materials through core spinning, in which roving of polyamide, polyester, or nylon is twisted around the elastane core fiber.[14,15] This core-spun structure, along with elastane's strong adhesion to sheath fibers[16] and resistance to most organic solvents, complicates the separation of these blended synthetic yarns and the recovery of individual materials at the end of their life cycle.[17] Standard mechanical recycling is ineffective for core-spun elastane, as it clogs machinery and hinders the recycling of sheath fibers.[18–20]

Neat elastane is incompatible with most other standard recycling methods.[18,19,21] Depolymerization, which breaks covalent bonds to recover monomers, is the most promising method for

[a]*Department of Materials Science and Engineering, Northwestern University, Evanston, IL, USA. E-mail: cchazot@northwestern.edu*
[b]*Institute of Bioproducts and Paper Technology, Graz University of Technology, Graz, Austria*
[c]*Department of Chemical Engineering, Northwestern University, Evanston, IL, USA*
[d]*Department of Chemical Engineering, Howard University, Washington, DC, USA*
†Electronic supplementary information (ESI) available. See DOI: https://doi.org/10.1039/d5lp00213c
‡These authors contributed equally to the work.

synthetic polymers similar to elastane, including polyurethanes.[22–24] While depolymerization can produce virgin-quality elastane,[19,23,25] it often results in downcycled products like small molecule lubricants that are not reinserted into the textile supply chain.[26,27] Depolymerization is also energy and time-intensive due to complex reaction pathways and challenging recovery of the reaction products.[28–30] Current limitations in recycling infrastructure mean that elastane-containing apparel must be discarded regardless of blend composition. Selective dissolution has shown promise for other blended textiles, like nylon–cotton, but elastane's limited solubility poses challenges.[17,31,32] Due to elastane's inherent chemical resistance, selective dissolution of elastane-containing blends typically targets the sheath fibers instead.[18,33] This process depends heavily on effective upstream composition sorting and often involves toxic solvent systems.[18,34,35] In rare cases where elastane is the target, such as in blends with polyamide,[21,34,36] complex solvent mixtures are required, which are incompatible with many other sheath materials. Moreover, most current efforts in selective dissolution focus on fiber removal rather than elastane recovery.[18,31,32,34,35,37] When recovery from solution is attempted, it often involves multistep solvent evaporation and thermal extrusion, processes that contribute 15% and 38% of the carbon footprint of recycling, respectively.[18] A blend-agnostic selective dissolution method that enables recovery of intact elastane fibers would significantly improve the scalability and sustainability of recycling strategies.

Here, we demonstrate that a dissolvable, biopolymeric interfacial coating can be applied to elastane fibers and subsequently dissolved to enable facile and universal separation of elastane fibers from blended textiles. The coating, based on naturally abundant chitosan (CS), is applied in a continuous roll-to-roll (R2R) dip-coating process, with its thickness being controlled by the concentration of biopolymer and viscosity of the bath. Through this process, a 5–10 μm CS coating can be conformally applied to 10-ply elastane fibers. We examine the effects of coating parameters on the morphology and thermo-mechanical properties of the CS-coated elastane fibers. Lastly, we demonstrate that coating dissolution in aqueous acidic conditions results in the recovery of elastane fibers.

Experimental

Materials

Chitosan (CS) was purchased from Millipore Sigma (low molecular weight-50 000–190 000 Da, 75–85% deacetylated, product number 448869) and used without further purification. To confirm purity and degree of deacetylation, ^{1}H NMR spectra were collected at room temperature using a Bruker Avance III HD 500 MHz spectrometer equipped with a BBO 5 mm Prodigy probe using CF3COOD (δ 11.50) as the solvent (Fig. S1 of the ESI†). The solubility parameter of CS was determined experimentally (Fig. S2†). Aqueous hydrochloric acid (0.5 N) was obtained from LabChem. Commercial-grade bare elastane fibers (105 denier) were used to evaluate the coating strategy on industrially relevant materials. These fibers, generously provided by The LYCRA Company, were used as received without further modification.

Methods

Preparation of the CS bath solution. CS baths of 2–7 weight percent (wt%) concentration were prepared as follows: the relevant mass of CS powder was first added to a 25 mL cup and 10 mL 0.5 N HCl was pipetted into the dry powder. The samples were then mixed in a planetary speed mixer (FlackTek DAC 330-100 PRO SpeedMixer) for two minutes at 2500 revolutions per minute (rpm) in ambient conditions. This mixing step was repeated after at least 10 minutes and again after one day to allow for the CS to swell and form a homogeneous solution. The total volume of the bath used for R2R operation was fixed at 20 mL to ensure consistent residence time of the fiber across all bath concentrations.

Roll-to-roll process. The R2R apparatus was designed and constructed in-house using custom-machined components. Elastane fibers were first spooled onto a stainless-steel sewing machine bobbin (the "spooling bobbin") using a benchtop bobbin winder. To operate the R2R apparatus, the virgin fiber was attached to the shaft of a NEMA 17 stepper motor, guided through the three-pulley system and manually wound a few times onto an empty identical bobbin (the "collecting bobbin"), also coupled to a NEMA 17 stepper motor. The two stepper motors were mounted 22 cm apart on a breadboard. The pulley mount, positioned to a vertical linear rail, was then lowered into the CS bath, and its height was fixed by tightening a set screw. Each stepper motor was controlled by an L298 stepper driver interfaced with an Arduino Uno. Rotational speed of the motors was maintained at 5 rpm, corresponding to a fiber linear speed average around 0.017 cm s^{-1} depending on bath viscosity and friction within the pulleys. A DC fan, powered separately, was pointed at the coated section of the fiber to induce drying.

Characterization

Coating thickness and morphology. Scanning electron microscopy (SEM-Hitachi SU8030) was used to observe cross-sections of coated and uncoated fibers. Prior to imaging, fibers were fractured using liquid nitrogen and coated with 18 nm of conductive osmium. Polarized optical microscopy (POM) was used to qualitatively probe coating uniformity (Nikon Eclipse LV100N-Pol Microscope, transmission mode, crossed polarization, quarter wave plate to differentiate elastane and CS coating).

Fourier-transform infrared spectroscopy (FTIR). FTIR was conducted on the CS powder and 10 cm of uncoated, coated, and HCl-immersed elastane fibers in the range of 400–4000 cm^{-1} (Bruker Alpha II Compact FTIR Spectrometer, Diamond ATR attachment). Water compensation and baseline correction were applied during data analysis. Peak integration was performed in Bruker OPUS, and results were normalized by calculating ratio of the peak of interest to a reference peak.

Thermal stability. Thermogravimetric analysis (TGA-Netzsch TG 209 F3 Taurus) was used to evaluate the amount of CS coated on elastane fibers. CS powder and the uncoated,

coated, and HCl-immersed elastane fibers were ramped from 75 to 650 °C at a rate of 20 °C min^{-1} and under a N_2 purge rate of 20 mL min^{-1}. The residual mass at 645 °C was used to assess the amount of CS deposited on elastane fibers.

Rheometry of bath solutions. Steady-shear flow curves were measured using a TA instruments HR-30 equipped with a 25 mm titanium plate and a Peltier plate to maintain the temperature at 25 °C. A solvent trap was used to prevent evaporation. The shear rate ranged from 0.1 to 200 s^{-1} with a 10 s equilibration time and a 10 s averaging time. These same conditions were performed on water to obtain the torque limit of the experimental setup. Data was excluded below the point at which the stress falls below the torque limit.

Mechanical testing. Uniaxial stress/strain curves and mechanical hysteresis data were collected for the uncoated and coated elastane fibers (Test Resources 510 E1 All Electric Dynamic Testing Machine). Samples were prepared at least 24 hours before testing. A gauge length of 12.5 mm and extension speed of 508 mm min^{-1} was used. The deformation profile of the mechanical testing consisted of five cycles of stretching the fiber to 300% strain, followed by the release of tension to allow for complete recovery of the fiber. On the fifth cycle, the fiber was held at 300% strain for 30 seconds to evaluate the decay in stress. The strain was then applied at the same extension speed for a sixth cycle, in which the fiber was stretched until failure (Fig. S3†).

Surface morphology. Atomic force microscopy (AFM) images of 10 × 10 μm^2 scan size were acquired using a Tosca™ 400 atomic force microscope (Anton Paar, Austria) in tapping mode. Silicon cantilevers (AP-ARROW-NCR from NanoWorld AG, Neuchatel, Switzerland) with a nominal force constant of 42 Nm^{-1} and tip radius of <10 nm were used. All measurements were conducted at room temperature. Of the untreated fibers and the fibers coated with 3, 5 and 7 wt%, at least two images per fiber were scanned on three different fibers, and representative images were selected. Image processing was performed with Gwyddion v2.58 software. Background subtraction was applied with a polynomial degree of two for all presented AFM images to improve the visualization of the surface and remove the fibers' natural curvature.

Redissolution of interfacial layer. To redissolve the CS layer, the coated fibers were placed directly into the HCl bath and stirred at 300 rpm for one hour. Samples were then dried in ambient conditions for 24 hours before further characterization.

Water resistance of interfacial layer. To test the durability of the CS coating in water, the coated fibers were submerged into a water bath and gently stirred for 30 seconds. Samples were then dried in ambient conditions for 24 hours before further characterization.

Results and discussion

Coating design and roll-to-roll implementation

First, we used Hansen solubility parameters (HSP) to select a relevant dissolvable interfacial coating polymer to enable facile and universal separation of elastane fibers from blended textiles (Fig. 1). To achieve this, the coating must satisfy the following criteria (Fig. 1a): (1) it must feature chemical compatibility with the elastane core and sheath fibers to enable sufficient adhesion; (2) it must be soluble in mild conditions that do not dissolve either elastane or the blended materials; and (3) it must be environmentally friendly and naturally abundant.[30] We followed Hansen's definition of the dispersive (δ_d), polar (δ_p), and hydrogen (δ_h) solubility parameter components such that the total solubility parameter is defined as:[38]

$$\delta_T = (\delta_d{}^2 + \delta_p{}^2 + \delta_h{}^2)^{\frac{1}{2}} \quad (1)$$

We then represented the interaction between CS, elastane, and relevant sheath fiber materials graphically (Fig. 1b), where $\delta_v = (\delta_d{}^2 + \delta_p{}^2)^{1/2}$ and δ_h were used as the axes. This 2D representation has been demonstrated as an effective way to visualize polymer–polymer interactions.[39] Compounds that feature strong interaction with a given polymer fall within a circular region centered on the solute coordinates (δ_v, δ_h) called the solubility circle. To satisfy criterion (1), the interfacial coating polymer solubility circle must overlap with that of both elastane and common synthetic sheath fibers, including polyamide 6,6 and polyester (*i.e.* polyethylene terephthalate). Among natural and abundant biopolymers, CS's solubility circle offers significant overlap with that of synthetic fibers of interest. CS contains hydroxyl and amino functional groups that enable strong hydrogen bonding with rigid urethane segments on the elastane backbone.[25,40–43] It is also soluble in dilute acidic solutions for a reasonable range of molecular weights, degrees of deacetylation, and concentrations, satisfying criterion (2).[40,44] Last, from a sustainability standpoint, CS is an attractive option due to its biodegradability and nontoxicity, satisfying criterion (3).[40,44,45] This polysaccharide has also demonstrated flame retardancy, a useful property in the garment industry.[46,47]

This preliminary analysis, in which CS was found to satisfy all three criteria based on HSP analysis and sustainability targets, guided our selection of CS dissolved in dilute aqueous HCl[48–50] as the bath solution for continuous dip-coating of elastane fibers.[51] To automate this process and underscore its scalability, we designed and built a benchtop roll-to-roll (R2R) apparatus (Fig. 1c). This setup was designed using a three-pulley system to guide a virgin elastane fiber into the CS bath solution, and then fan-dry the coating before winding the coated fiber onto a clean bobbin. By setting a constant winding speed and bath residence time, and adjusting for uniform fiber tension, we successfully coated elastane fibers in a bath containing 4–7 wt% CS, as observed in SEM cross-sections (Fig. 1d). The 5–10 μm CS interface layer conformally wraps and compresses the plies, suggesting a strong chemical interaction with elastane, as predicted by HSP analysis.

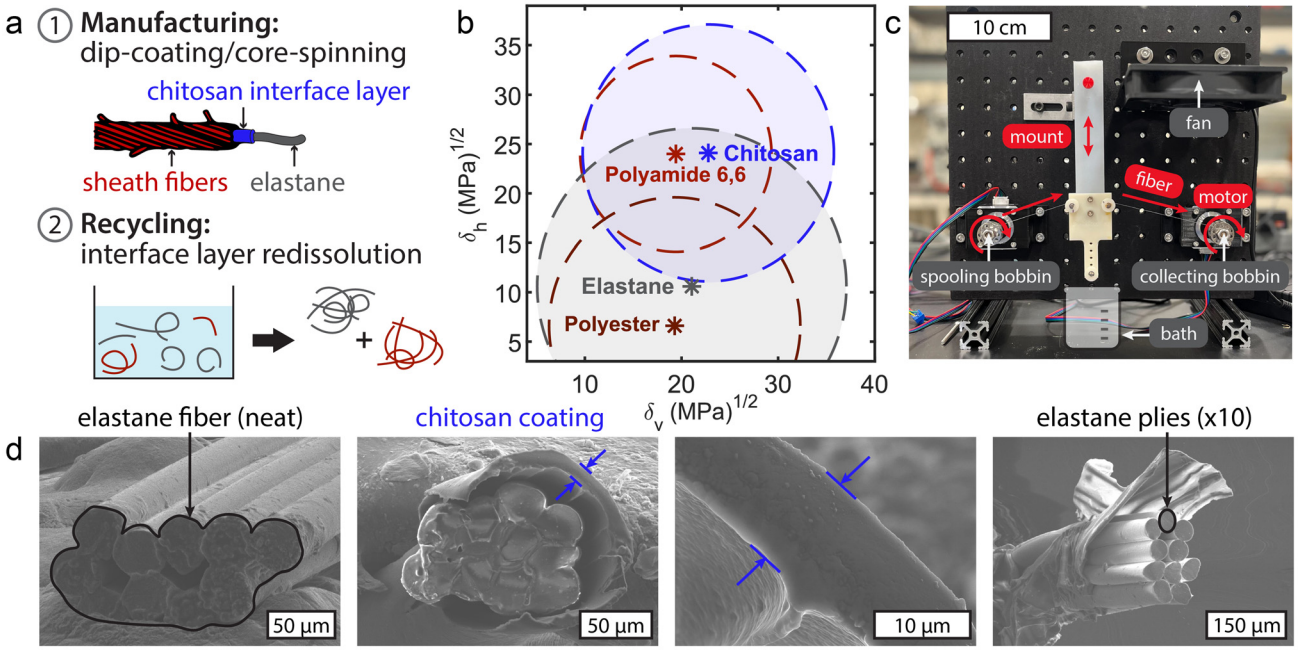

Fig. 1 (a) Illustration of the elastane fiber with the dip-coated chitosan (CS) layer as interface between the elastane and the sheath fibers to improve recycling *via* interface layer redissolution. (b) Hansen solubility plot of relevant textile polymer fibers and CS. (c) Roll-to-roll (R2R) pulley system applied in this work. The elastane fiber is guided into the CS bath, and then a fan is used to induce drying of the coated fiber. (d) Several SEM images illustrating the elastane fiber, which is a bundle of 10 single filaments (plies), successfully coated with CS.

Influence of bath concentration on CS content and interaction

With the continuous R2R process established, we investigated the impact of CS concentration and bath rheology on coating thickness (Fig. 2).[51,52] CS-HCl solutions exhibit distinct rheological regimes depending on polymer concentration (also denoted as "bath conc."), each characterized by varying degrees of shear thinning (Fig. 2a). In the first regime (bath conc. < 0.75 wt%), the solutions are Newtonian. As concentration increases, the solution transitions from the dilute to semi-dilute regime. This transition corresponds to a logarithmic increase in zero-shear viscosity η_0 (Fig. 2b) and stronger shear-thinning. We found that only baths with CS concentrations in the semi-dilute regime (3–7 wt%, our processing window) resulted in the formation of a CS coating on elastane.

The formation of a CS coating was further confirmed by TGA (Fig. 2c and d). The presence of the CS coating is qualitatively supported by the characteristic shape of the mass loss curves (Fig. 2c). Increasing the CS bath concentration leads to a decrease in the onset decomposition temperature. Additionally, the residual mass at 645 °C provides further evidence of increased coating thickness with higher bath concentrations (Fig. 2d). Pure CS had a residual mass of around 40%, while neat elastane had a residual mass below 3% (Fig. 2c). As CS bath concentration increases from 3 to 6 wt%, the average residual mass of the coated fibers triples, denoting a corresponding increase in coating thickness (Fig. 2d). Bath concentrations below 3 wt% resulted in no significant residual mass increase compared to neat elastane, likely due to their low capillary number and the resulting absence of CS coating.[53] We also observed a plateau in residual mass for CS bath concentrations above 6 wt%, attributed to the formation of a non-uniform beaded coating due to significant non-Newtonian flow effects or air entrainment.[53,54] These residual mass results also demonstrate that CS coating can enhance flame retardancy of elastane fibers, a useful property for performance textiles.

FTIR spectroscopy was used to provide further evidence of successful CS coating and probe chemical interaction between CS and elastane (Fig. 2e, f and Fig. S4†). In the virgin elastane spectrum, there is a sharp peak at 1102 cm^{-1} followed by a lower-intensity shoulder (between 900 and 1030 cm^{-1}) corresponding to the C–O (ether) bond.[55] In pure CS, a strong, broad absorption peak between 800 and 1220 cm^{-1} is present and characteristic of C–O–C in the CS saccharide repeat unit.[56] We noted an increase in absorption intensity within this characteristic CS region as the bath concentration increased, particularly along the lower wavenumber edge of the investigated range (below 1000 cm^{-1}) (Fig. 2e). Integrating the relevant broad aggregate peak (between 900 cm^{-1} and 1170 cm^{-1}) and normalizing by a vibrational signature only present in the elastane signal (from 1685 to 1760 cm^{-1}, comprising the amide I and ester vibrational modes) further confirms the increase in CS coating thickness with bath concentration in the range of 3 to 5 wt% (Fig. 2f and Fig. S4†). Fibers coated with 6 and 7 wt% CS solutions showed a lower characteristic CS signal, likely due to coating non-uniformity. Fibers with a thin CS coating (4–5 wt% bath concentration) featured an amplified intensity

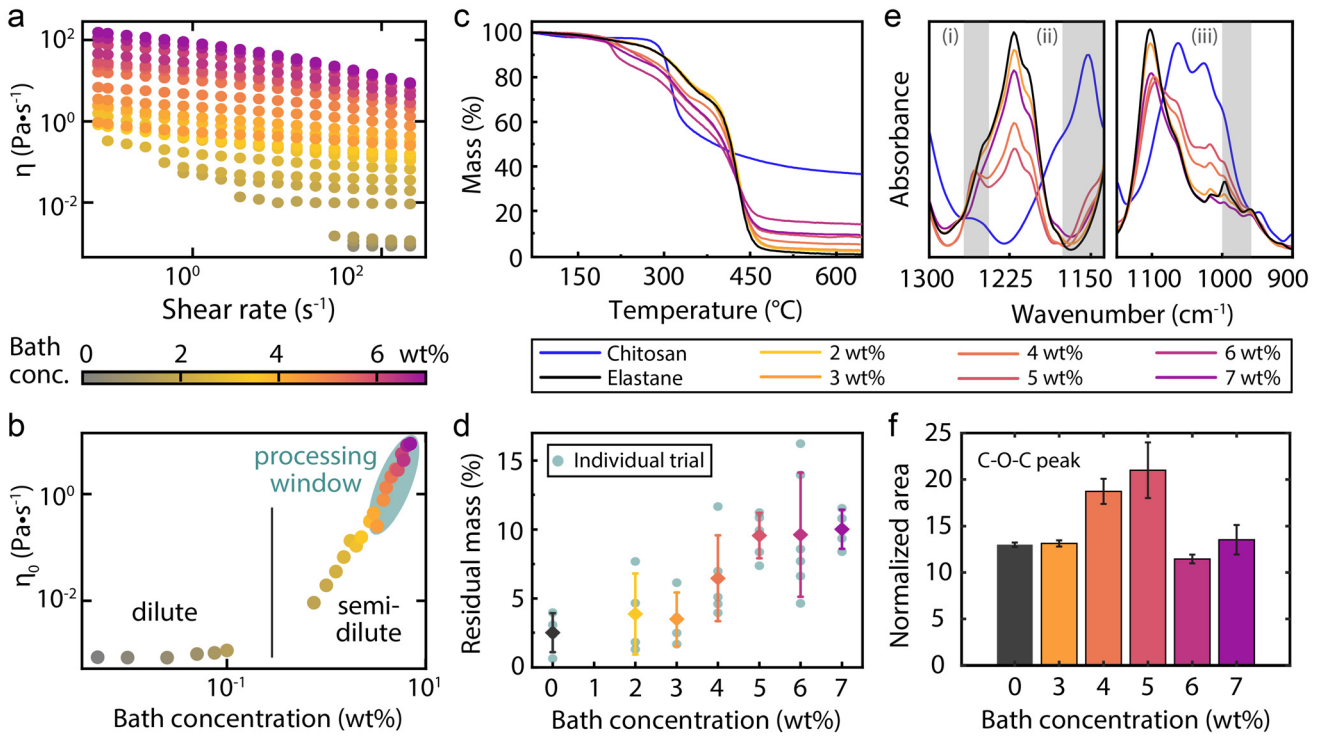

Fig. 2 (a) Flow curves for 25 concentrations between 0 and 7 wt% CS in aqueous 0.5 N HCl. (b) Associated zero-shear viscosity which highlights the dilute regime, semi-dilute regime, and processing window for the bath concentrations. (c) TGA curves for CS, virgin elastane fiber, and coated elastane fibers (2–7 wt% bath concentrations). (d) Average residual mass of fibers in TGA experiment at 645 °C. (e) Overlayed FTIR spectra for 3 wt%, 4 wt%, 5 wt%, 7 wt% coated fibers, virgin elastane, and CS in two regions of interest: 1300–1135 cm^{-1}, and 1170–900 cm^{-1}. These regions encompass the CH_2 (CS) bend at 1258 cm^{-1} (i), the C–O–C (CS) stretch at 1150 cm^{-1} (ii), and the broad absorption peak for C–O–C (CS) below 1000 cm^{-1} (iii). (f) Ratio of the calculated area of the C–O–C peak in the 1170–900 cm^{-1} region to the reference peak in the 1685 to 1760 cm^{-1} region for 3 wt%, 4 wt%, 5 wt%, 6 wt%, and 7 wt% coated fibers.

for vibrational modes characteristic of the pyranose ring of CS (CH_2 bending at 1258 cm^{-1} and asymmetric stretching of the C–O–C bridge at 1150 cm^{-1}) (Fig. 2e).[57,58] This suggests significant molecular interaction between CS and elastane, in turn affecting the vibrational degrees of freedom of the saccharide units and their amplitude.[57] Fibers coated in high-viscosity 6 and 7 wt% solutions do not show the same vibrational mode modulation due to coating heterogeneities and potential decrease of CS-elastane intermolecular interaction at large coating thicknesses.

Mechanical properties of the coated fibers

We then evaluated the effect of the dip-coating process and CS coating on elastane's copolymer structure and mechanical performance. Preservation of crystallinity after dip-coating treatment was confirmed by WAXS, comparing the spectra for virgin elastane, 4 wt%, and 7 wt% coated fibers (Fig. S5†). This suggests that exposure to HCl did not affect the elastane copolymer morphology and crystalline domains. Using a standardized cyclic tensile testing procedure, we assessed the impact of CS coating thickness on reversible stretchability under uniaxial periodic strain (Fig. 3 and Fig. S3†).

Elastane fibers show a large hysteresis under cyclic load, both in the presence and absence of CS coating.[59,60] The CS coating appears to significantly affect the shape of the first load cycle, with sudden stress drops at large CS bath concentrations (Fig. 3a). Evaluating the elastic modulus for the initial slope of the first tensile load resulted in average values which are between 5 and 15 MPa, with a slight decrease with the addition of a CS coating (Fig. 3b). However, these values were calculated by neglecting variations of cross-sectional area and CS coating thickness between fibers. These variations are likely the source of the slight differences observed in elastic modulus.

Hysteresis is an indication of the energy dissipated in the fiber during one loading-unloading cycle. In elastane fibers, the dissipated energy of the first cycle is about three times larger than in subsequent cycles (Fig. 3c). Comparing the energy dissipated across the CS bath concentration range, the values are very similar for the 3–4 wt% coated fibers, which exhibited slightly higher values in every cycle, while the 5–6 wt% coated fibers have lower or unchanged values compared to the uncoated fibers. Only the 7 wt% coated fibers showed stronger deviations, with higher dissipation values than the uncoated fibers in cycles 1–4. Moreover, in cycle 1, several instant drops in stress are observed at higher strain values in 7 wt% coated fibers (Fig. 3a). Macroscopic observations of individual ply failure at stress drops suggest that

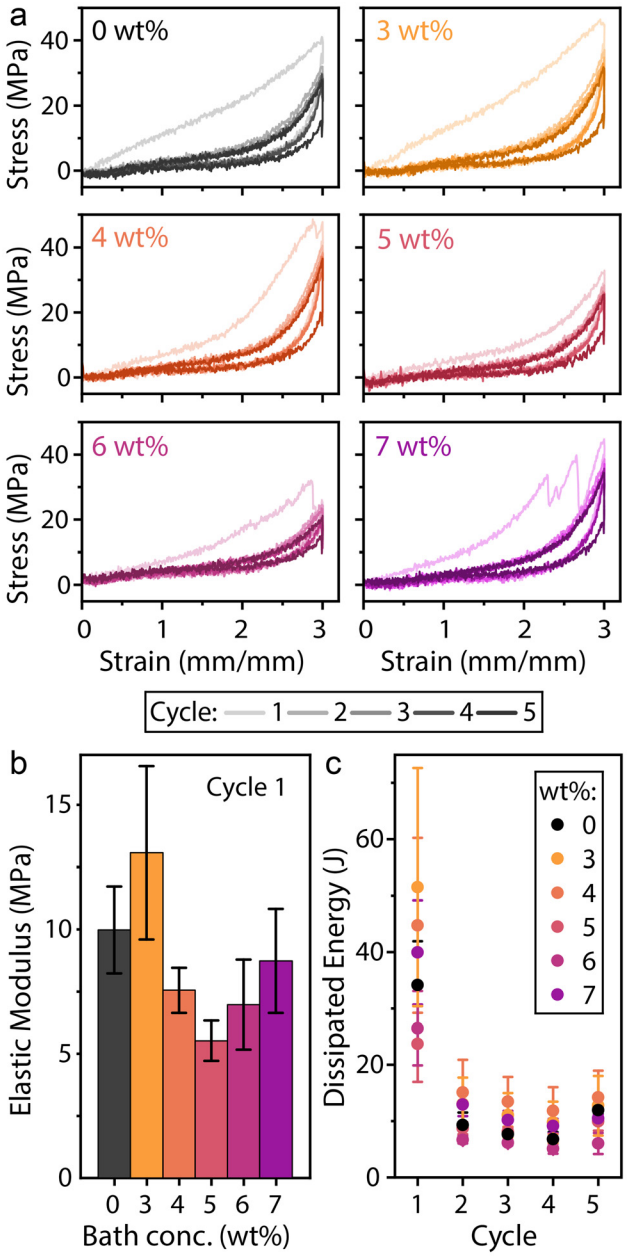

Fig. 3 (a) Stress–strain diagrams from cyclic tensile testing of the CS-coated elastane fibers at different CS concentrations (0 wt%, 3 wt%, 4 wt%, 5 wt%, 6 wt%, and 7 wt%) performed for 5 hysteresis cycles. (b) Results of the elastic modulus determined from the first cycle for the different CS concentrations. (c) Dissipated energy obtained for each cycle for the different CS concentrations by calculating area under the hysteresis curves.

immersion in a high-viscosity 7 wt% bath solution results in decreased ply interaction and fiber weakening during the coating process.

Although CS and elastane have good chemical compatibility for adhesion, there seems to be a mechanical mismatch between the two materials. CS exhibits wide-ranging mechanical properties (*e.g.*, tensile strength values range from a few MPa to 100 MPa), which are tunable to a certain degree by processing and additives.[61] In direct comparison to elastane, which exhibits typical values of 1 MPa for tensile strength and up to 10 MPa for elastic modulus, CS is significantly stiffer and more brittle.[62] In most cases, CS-based films and fibers have an elongation at break below 50%, whereas elastane reaches stretchability values of up to 600% due to its thermoplastic elastomeric nature.[61,63] Therefore, it is surprising that coating elastane with CS does not lead to a significant increase in elastic modulus or decrease in dissipated energy. Observed coating lift-off, fracture, and ply separation under mechanical stress suggest that the strong mechanical property mismatch dominated the observed tensile properties, resulting in decreased macroscale adhesion despite strong intermolecular hydrogen bonding.

However, a quantified description of the mechanical behavior of neat and coated elastane is complicated by variations in the fibers' structural arrangement. The elastane fibers featured ten individual plies solely interacting through weak physical or electrostatic interactions. Therefore, stretching the whole elastane fiber assembly can induce reorientation and shifting of the plies into different packing geometries. We observed this rearrangement through optical microscopy of microtome-sectioned longitudinal slices taken at multiple positions along several centimeters of a continuous elastane fiber (Fig. S6†). This geometric reorganization of the plies likely occurs during the R2R dip-coating process of fibers under tension, particularly in high viscosity solutions (*e.g.*, 6–7 wt% bath conc.). Overall, mechanical property characterization indicates that the dip-coating process has minimal effect on elastane's stretchability. However, high bath viscosity can significantly influence the stretched state and cross-sectional area of coated elastane fibers, affecting failure modes. The impact of dip-coating on ply configuration was further evaluated through direct morphological analysis of CS-coated fibers (Fig. 4). Low magnification POM observation of the CS-coated fibers revealed that the 4 wt% coated fibers have an intact thin CS coating, while the 5–7 wt% coated fibers showed varied coating thickness, along with CS fracture and delamination along the fiber length (Fig. 4a). For a bath concentration of 7 wt%, regions where the coating is still intact showed significant compression of the elastane core in comparison to uncoated sections. Heterogeneities in the CS coating along the fiber direction are also accompanied by changes in coating surface morphology, as measured by AFM (Fig. 4b). Whereas the uncoated fiber exhibited the anisotropic linear pattern typical of the surface of spun synthetic fibers, the surface morphology evolves with increasing coating thickness. At 3 wt% and 5 wt%, the surface appeared homogeneously and conformally coated, as evidenced by the presence of the linear pattern from the underlying elastane fiber. However, fibers finished in 7 wt% solutions exhibit lateral cracks of several μm in length within the CS coating. In summary, elastane fibers finished using bath concentrations of 4–5 wt% featured the most uniform CS coating with no significant impact on the stretchability, failure mechanism, and ply morphology compared to neat elastane.

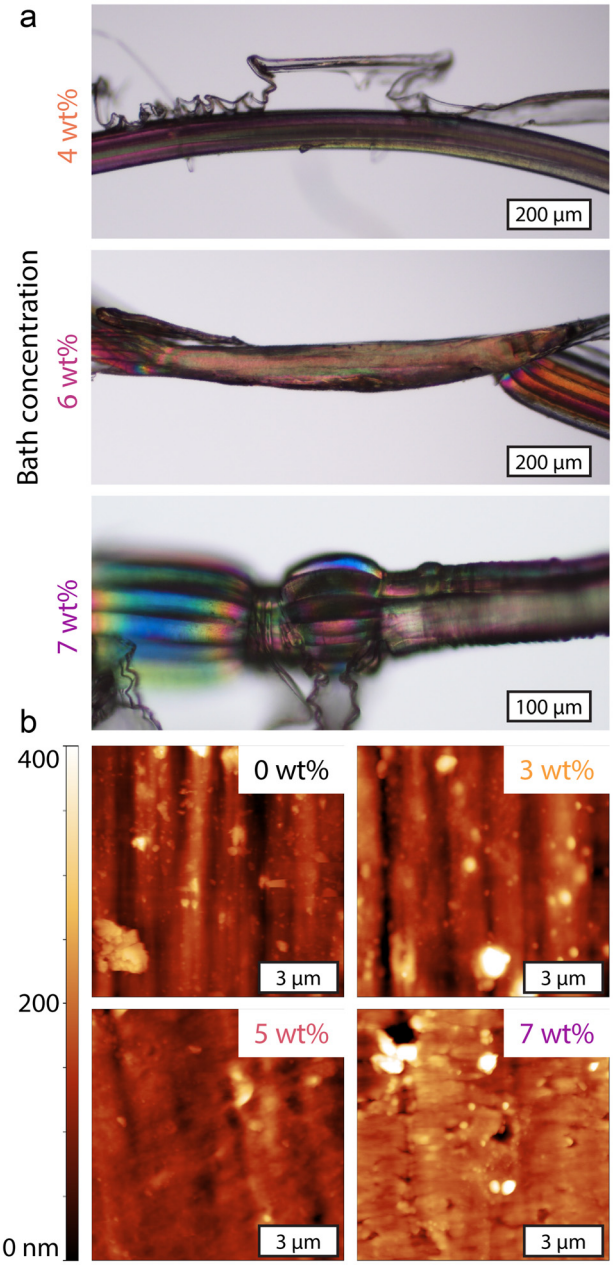

Fig. 4 (a) POM images of 4 wt%, 6 wt%, and 7 wt% bath concentrations demonstrating adherence of the CS coating to the fiber. (b) Representative 10 × 10 µm^2 AFM topography images (*z*-scale: 400 nm) for 0 wt%, 3 wt%, 5 wt%, and 7 wt% bath concentrations.

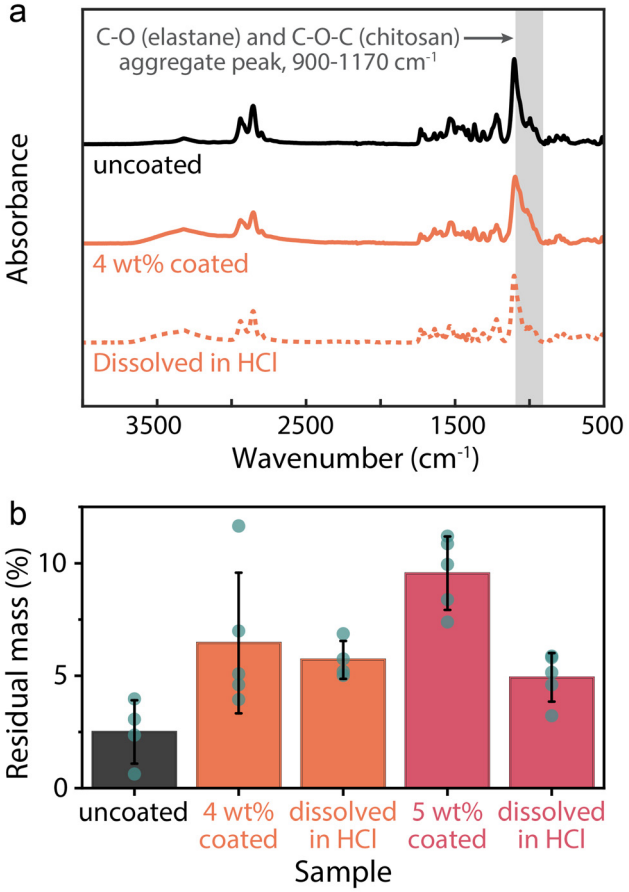

Fig. 5 (a) Representative FTIR spectra of virgin elastane, 4 wt% coated fiber, and 4 wt% fiber immersed in aqueous HCl. The region of interest is highlighted. (b) Residual mass from TGA curves, calculated for virgin elastane and 4–5 wt% coated fibers before and after immersion in HCl. Small circular data points represent individual trials.

Selective dissolution of CS coating

We tested the chemical resistance of the 4 and 5 wt% coated fibers by selective dissolution of CS in aqueous 0.5 N HCl (Fig. 5). Elastane fibers were successfully recovered from the HCl bath without visible damage or ply separation. FTIR analysis confirmed that the coating dissolution did not induce significant changes in the chemical structure of the elastane (Fig. 5a). Additionally, partial dissolution of the coating was evident from a reduction in the C–O–C stretching signal, characteristic of the CS layer, following immersion. These FTIR spectra exhibited no notable differences in the region of interest between the 4 wt% and 5 wt% CS coatings (Fig. S7†). Interestingly, TGA conducted on fibers treated with HCl for CS removal only showed a decrease in residual mass after coating dissolution for the 5 wt% coated fibers, while the 4 wt% coated fibers showed no change (Fig. 5b). Combined with the FTIR analysis in Fig. 2e and f, we expect that the chemical interaction between the CS coating and elastane fiber is stronger for thinner coatings (*i.e.*, bath solutions of lower concentration) due to enhanced adhesion *via* hydrogen bonding interactions. After immersion in HCl, most of the 4 wt% coating stays intact, while the outer layer of the 5 wt% coating is expected to be redissolved. Furthermore, both the 4 wt% and 5 wt% coated fibers exhibited higher residual mass than the neat fibers, likely due to CS residue firmly adhering to the elastane surface. Thus, once a certain coating thickness is reached with the 4 wt% bath, additional CS appears to adhere less effectively. Overall, we showed that selective coating dissolution can enable the recovery of elastane fibers with minimal residual CS adhered to the surface. The balance

between coating thickness and adhesion can be tailored to enhance recyclability *via* selective dissolution or to improve chemical resistance for further textile processing, such as dyeing.

Conclusions

We have designed and demonstrated the conformal coating of elastane fibers with CS, an abundant natural polymer that can be selectively dissolved to facilitate neat elastane recovery. We implemented the method in a pilot-scale roll-to-roll dip-coating apparatus and studied the impact of bath concentration and viscosity on coating morphology. CS bath concentrations of 4–5 wt% resulted in a uniform coating with the best adhesion to the elastane core. We demonstrated that the CS coating did not impair elastane's stretchability and that it enhanced the thermal stability of the resulting fibers. Lastly, we demonstrated how adjusting the thickness and spatially resolved intermolecular interactions can tailor the chemical resistance of the CS finishing layer. This enables selective coating dissolution under acidic conditions, allowing elastane fibers to be recovered without detectable mechanical or chemical degradation.

Further improvement in adhesion could be achieved by decreasing the mechanical mismatch between CS and elastane or enhancing hydrophobicity. Indeed, preliminary testing of the water resistance of the 4–5 wt% coatings and subsequent analysis by FTIR (Fig. S7†) suggests that immersion in deionized water for as little as 30 seconds may result in some coating loss (Fig. S8†). This redissolution behavior at neutral pH could pose challenges for textile durability during regular washing. This issue could be addressed by incorporating more hydrophobic biopolymers into the coating or by refining processing conditions during the finishing steps. For example, the current coating strategy does not include an acid neutralization step, which may improve the water resistance of the CS layer. Surface pretreatments commonly applied to cotton and polyesters (*e.g.*, silanization and UV/ozone plasma) could also be adapted to elastane.[64,65] Additionally, tuning fiber velocity to increase the capillary number during coating may enhance adhesion.[53]

Beyond addressing these practical considerations, this work serves as a proof-of-concept for scalable elastane finishing with improved recovery upon selective dissolution. It also offers critical insights into the balance of CS-elastane molecular interactions and mechanical property mismatches leading to uniform coating formation and property enhancement. The design principles and fundamental knowledge generated here can be leveraged to explore other relevant biopolymers, such as cellulose ethers and acetates, as dissolvable interface layers for textile recycling. This advancement broadens the applicability of the demonstrated fiber finishing and selective coating dissolution methods, paving the way for innovative recycling solutions for a wide range of blended fibers and textiles.

Author contributions

C. A. C. C., E. C. G. and M. C. conceptualized the research. C. A. C. C. supervised the research. G. W. conducted preliminary work leading to the results presented here. M. C. built the R2R apparatus. M. C., E. C. G. and N. F. conducted fiber coating/redissolution experiments. E. S. and M. C. conducted SEM imaging. M. C. and E. C. G. conducted FTIR measurements. M. C., C. C., J. S. and E. C. G. conducted mechanical testing and analysis. S. B. and C. A. C. C. conducted TGA. K. T. G. conducted rheometry under the supervision of J. J. R., E. C.G., C. C. and N. F. conducted POM imaging. E. C. G. and M. C. wrote the first draft of the manuscript. C. A. C. C. edited the manuscript and oversaw its writing. All authors commented on the manuscript.

Conflicts of interest

There are no conflicts to declare.

Data availability

The FTIR, TGA, and stress/strain data supporting this study are available at: E. C. Grosvenor, M. Cohen, & C. A. C. Chazot (2025). A roll-to-roll chitosan finishing strategy for elastane recovery [Data set]. Northwestern University. **https://doi.org/10.5281/zenodo.15863582.**

Acknowledgements

This work was primarily funded through the Northwestern University (NU) Materials Research Science and Engineering Center (NU-MRSEC), through the Academic-Year Undergraduate Research Internship (URI) program supporting M. C. and E. S., the Research Experience for Undergraduates (REU) program supporting G. W., and a seed grant awarded to C. A. C. C. supporting S. E. B. (National Science Foundation – NSF Award Number DMR-2308691). G. W. was also supported through the Materials Initiative for Comprehensive Research Opportunity (MICRO) at NU. MICRO is generously supported by an unrestricted gift from the 3M Foundation awarded to C. A. C. C. (3M STEM and Skilled Trades Program). E. C. G. was supported through the NSF Graduate Research Fellowship Program (GRFP – Award Number DGE-2234667). K. G. was supported through an NSF CAREER Award (Award Number CBET-2047365) awarded to J. J. R. and a seed grant awarded to C. A. C. C. and J. J. R. by the Paula M. Trienens Institute for Sustainability and Energy. C. C. was supported through a seed grant awarded to C. A. C. C. by the International Institute for Nanotechnology (IIN). This work also made use of the NUANCE and EPIC facilities for sample preparation and imaging; the Jerome B. Cohen X-Ray Diffraction Facility for X-ray diffraction experiments; the

CLaMMP Facility for mechanical testing; and the IMSERC NMR Facility. NUANCE Center has received support from the SHyNE Resource (NSF ECCS-2025633), the IIN, and Northwestern's MRSEC program (NSF DMR-2308691). The CLaMMP Facility has received support from the MRSEC Program (NSF DMR-1720139), the Center for Hierarchical Materials Design, and from Northwestern University. IMSERC (RRID:SCR_017874) NMR Facility has received support from the SHyNE Resource (NSF ECCS-2025633), the IIN, and Northwestern University. The authors thank Hong Liu from The LYCRA Company for providing fibers and valuable insights on handling and testing of elastane. We would also like to thank Sumit Kewalramani for his guidance with WAXS testing, and Ayesha Anis for her work on characterization of chitosan.

References

1 Materials Market Report 2024, https://textileexchange.org/knowledge-center/reports/materials-market-report-2024/, (accessed December 2024).
2 A. Bartl and W. Ipsmiller, Fast fashion and the Circular Economy: Symbiosis or antibiosis?, *Waste Manage. Res.*, 2023, **41**, 497–498.
3 K. Niinimäki, G. Peters, H. Dahlbo, P. Perry, T. Rissanen and A. Gwilt, The environmental price of fast fashion, *Nat. Rev. Earth Environ.*, 2020, **1**, 189–200.
4 E. Peter John and U. Mishra, A sustainable three-layer circular economic model with controllable waste, emission, and wastewater from the textile and fashion industry, *J. Cleaner Prod.*, 2023, **388**, 135642.
5 A New Textiles Economy: Redesigning fashion's future, https://www.ellenmacarthurfoundation.org/a-new-textiles-economy, (accessed December 2024).
6 T. Lewis, Apparel disposal and reuse, in *Sustainable Apparel*, ed. R. Blackburn, Woodhead Publishing, 2015, pp. 233–250.
7 16 CFR § 303.7 - Generic names and definitions for manufactured fibers. LII/Legal Information Institute, https://www.law.cornell.edu/cfr/text/16/303.7, (accessed January 2025).
8 G. Gorrasi, M. Tortora and V. Vittoria, Synthesis and physical properties of layered silicates/polyurethane nanocomposites, *J. Polym. Sci., Part B:Polym. Phys.*, 2005, **43**, 2454–2467.
9 H. Zhang, Y. Chen, Y. Zhang, X. Sun, H. Ye and W. Li, Synthesis and Characterization of Polyurethane Elastomers, *J. Elastomers Plast.*, 2008, **40**, 161–177.
10 K. Singha, Analysis of Spandex/Cotton Elastomeric Properties: Spinning and Applications, *Int. J. Compos. Mater.*, 2012, **2**, 11–16.
11 M. N. Hassan, M. Rokonuzzaman, A. Razzaque, A. Rahim, A. Hossain and T. Islam, Effect of spandex linear density and twist multiplier on the properties of core spun yarn and denim fabric, *SPE Polym.*, 2024, **5**, 610–623.
12 H. Kanai, K. Ogawa, T. Sasagawa and K. Shibata, Influence of the mechanical stretch property of fabrics on the wear comfort of men's suit pants, *Text. Res. J.*, 2021, **91**, 2771–2785.
13 N. Ozdil, Stretch and Bagging Properties of Denim Fabrics Containing Different Rates of Elastane, *Fibres Text. East. Eur.*, 2008, **16**, 66.
14 H. X. Zhang, Y. Xue and S. Y. Wang, Effects of twisting parameters on characteristics of rotor-spun composite yarns with spandex, *Fibers Polym.*, 2006, **7**, 66–69.
15 O. Babaarslan, Method of Producing a Polyester/Viscose Core-Spun Yarn Containing Spandex Using a Modified Ring Spinning Frame, *Text. Res. J.*, 2001, **71**, 367–371.
16 R. Rathinamoorthy, S. Raja Balasaraswathi, S. Madhubashini, A. Prakalya, J. B. Rakshana and S. Shathvika, Investigation on microfiber release from elastane blended fabrics and its environmental significance, *Sci. Total Environ.*, 2023, **903**, 166553.
17 Y. Yin, D. Yao, C. Wang and Y. Wang, Removal of spandex from nylon/spandex blended fabrics by selective polymer degradation, *Text. Res. J.*, 2014, **84**, 16–27.
18 K. Phan, S. Ügdüler, L. Harinck, R. Denolf, M. Roosen, G. O'Rourke, *et al.*, Analysing the potential of the selective dissolution of elastane from mixed fiber textile waste, *Resour., Conserv. Recycl.*, 2023, **191**, 106903.
19 D. Achilias, L. Andriotis, I. Koutsidis, D. Louka, N. Nianias, P. Siafaka, I. Tsagkalias, and G. Tsintzou, Recent Advances in the Chemical Recycling of Polymers (PP, PS, LDPE, HDPE, PVC, PC, Nylon, PMMA), in *Material Recycling - Trends and Perspectives*, ed. D. Achilias, InTech, 2012, DOI: 10.5772/33457.
20 K. Choudhury, M. Tsianou and P. Alexandridis, Recycling of Blended Fabrics for a Circular Economy of Textiles: Separation of Cotton, Polyester, and Elastane Fibers, *Sustainability*, 2024, **16**(14), 6206.
21 E. Boschmeier, A. Bartl and A. Vasiliki-Maria, New separation process for elastane from polyester/elastane and polyamide/elastane textile waste, *Resour., Conserv. Recycl.*, 2023, **198**, 107215.
22 R. B. Baloyi, O. J. Gbadeyan, B. Sithole and V. Chunilall, Recent advances in recycling technologies for waste textile fabrics: a review, *Text. Res. J.*, 2024, **94**, 508–529.
23 S. L. Loo, E. Yu and X. Hu, Tackling critical challenges in textile circularity: A review on strategies for recycling cellulose and polyester from blended fabrics, *J. Environ. Chem. Eng.*, 2023, **11**, 110482.
24 W. H. Xu, L. Chen, S. Zhang, R. C. Du, X. Liu, S. Xu, *et al.*, New insights into urethane alcoholysis enable chemical full recycling of blended fabric waste, *Green Chem.*, 2023, **25**, 245–255.
25 T. Duhoux, E. Maes, M. Hirschnitz-Garbers, K. Peeters and L. Asscherickx, *et al.*, *Study on the technical, regulatory, economic and environmental effectiveness of textile fibres recycling: final report*, Publications Office of the European Union, 2021, https://data.europa.eu/doi/10.2873/828412 (accessed January 2025).

26 L. Korley, T. Epps III, B. Helms and A. Ryan, Toward polymer upcycling—adding value and tackling circularity, *Science*, 2021, **373**, 66–69.
27 ReHubs: A joint initiative for industrial upcycling of textile waste streams & circular materials, **https://euratex.eu/wp-content/uploads/Recycling-Hubs-FIN-LQ.pdf** (accessed January 2025).
28 H. Wu, B. Wang, T. Li, Y. Wu, R. Yang, H. Gao, *et al.*, Efficient recycle of waste poly-cotton and preparation of cellulose and polyester fibers using the system of ionic liquid and dimethyl sulfoxide, *J. Mol. Liq.*, 2023, **388**, 122757.
29 M. Kahoush and N. Kadi, Towards sustainable textile sector: Fractionation and separation of cotton/polyester fibers from blended textile waste, *Sustainable Mater. Technol.*, 2022, **34**, e00513.
30 C. A. C. Chazot, Disentangling Current Challenges to Weave the Future of Sustainable Textiles, *Acc. Mater. Res.*, 2023, **4**, 385–388.
31 L. Villar, I. Schlapp-Hackl, P. B. Sánchez and M. Hummel, High-Quality Cellulosic Fibers Engineered from Cotton–Elastane Textile Waste, *Biomacromolecules*, 2024, **25**, 1942–1949.
32 L. Wang, S. Huang and Y. Wang, Recycling of Waste Cotton Textile Containing Elastane Fibers through Dissolution and Regeneration, *Membranes*, 2022, **12**(4), 355.
33 M. Zhu, C. Gao, S. Wang, S. Shi, M. Zhang and Q. Su, Recycling of Spandex: Broadening the Way for a Complete Cycle of Textile Waste, *Sustainability*, 2025, **17**(8), 3319.
34 L. Vonbrül, M. Cordin, A. P. Manian, T. Bechtold and T. Pham, Solvent blends for selective elastane dissolution and recovery from mixed polyamide fabrics, *Resour., Conserv. Recycl.*, 2024, **200**, 107302.
35 C. Gong, K. Zhang, C. Yang, J. Chen, S. Zhang and C. Yi, Simple process for separation and recycling of nylon 6 and polyurethane components from waste nylon 6/polyurethane debris, *Text. Res. J.*, 2021, **91**, 18–27.
36 M. B. Johansen, B. S. Donslund, M. L. Henriksen, S. K. Kristensen and T. Skrydstrup, Selective chemical disassembly of elastane fibres and polyurethane coatings in textiles, *Green Chem.*, 2023, **25**, 10622–10629.
37 E. Boschmeier, D. Mehanni, V. L. Sedlmayr, Y. Vetyukov, S. Mihalyi, F. Quartinello, *et al.*, Recovery of pure PET from wool/PET/elastane textile waste through step-wise enzymatic and chemical processing, *Waste Manage. Res*, 2025, **43**, 969–979.
38 C. Hansen, *Hansen Solubility Parameters: A User's Handbook*, CRC Press, Boca Raton, FL, 2nd edn, 2007.
39 D. Van Krevelen and K. Te Nijenhuis, *Properties of Polymers, Chapter 7: Cohesive Properties and Solubility, in* Elsevier, Amsterdam, 2009, pp. 189–227.
40 M. Hayes, Chitin, Chitosan and their Derivatives from Marine Rest Raw Materials: Potential Food and Pharmaceutical Applications, in *Marine Bioactive Compounds: Sources, Characterization and Applications*, ed. M. Hayes, Springer US, Boston, MA, 2012, pp. 115–128.
41 S. Trujillo, E. Pérez-Román, A. Kyritsis, J. L. Gómez Ribelles and C. Pandis, Organic–inorganic bonding in chitosan–silica hybrid networks: Physical properties, *J. Polym. Sci., Part B:Polym. Phys.*, 2015, **53**, 1391–1400.
42 B. YuM, R. Lya, V. N. Nikitin and N. P. Apukhtina, A study of hydrogen bonding in urethane elastomers by infrared spectroscopy, *Polym. Sci. U.S.S.R.*, 1965, **7**, 859–867.
43 H. S. Lee, J. H. Ko, K. S. Song and K. H. Choi, Segmental and chain orientational behavior of spandex fibers, *J. Polym. Sci., Part B:Polym. Phys.*, 1997, **35**, 1821–1832.
44 V. K. Thakur and M. K. Thakur, Recent Advances in Graft Copolymerization and Applications of Chitosan: A Review, *ACS Sustainable Chem. Eng.*, 2014, **2**, 2637–2652.
45 C. P. Jiménez-Gómez and J. A. Cecilia, Chitosan: A Natural Biopolymer with a Wide and Varied Range of Applications, *Molecules*, 2020, **25**(17), 3981.
46 Y. Pan and H. Zhao, A novel blowing agent polyelectrolyte for fabricating intumescent multilayer coating that retards fire on cotton fabric, *J. Appl. Polym. Sci.*, 2018, **135**, 46583.
47 L. Liu, Y. Pan, Z. Wang, Y. Hou, Z. Gui and Y. Hu, Layer-by-Layer Assembly of Hypophosphorous Acid-Modified Chitosan Based Coating for Flame-Retardant Polyester–Cotton Blends, *Ind. Eng. Chem. Res.*, 2017, **56**, 9429–9436.
48 J. Wu and L. Zhang, Dissolution behavior and conformation change of chitosan in concentrated chitosan hydrochloric acid solution and comparison with dilute and semidilute solutions, *Int. J. Biol. Macromol.*, 2019, **121**, 1101–1108.
49 Q. x. Li, B. z. Song, Z. q. Yang and H. l. Fan, Electrolytic conductivity behaviors and solution conformations of chitosan in different acid solutions, *Carbohydr. Polym.*, 2006, **63**, 272–282.
50 A. Narkevicius, L. M. Steiner, R. M. Parker, Y. Ogawa, B. Frka-Petesic and S. Vignolini, Controlling the Self-Assembly Behavior of Aqueous Chitin Nanocrystal Suspensions, *Biomacromolecules*, 2019, **20**, 2830–2838.
51 J. Park, K. Shin and C. Lee, Roll-to-Roll Coating Technology and Its Applications: A Review, *Int. J. Precis. Eng. Manuf.*, 2016, **17**, 537–550.
52 R. Runser, S. E. Root, D. E. Ober, K. Choudhary, A. X. Chen, C. Dhong, *et al.*, Interfacial Drawing: Roll-to-Roll Coating of Semiconducting Polymer and Barrier Films onto Plastic Foils and Textiles, *Chem. Mater.*, 2019, **31**, 9078–9086.
53 T. D. Blake, R. A. Dobson and K. J. Ruschak, Wetting at high capillary numbers, *J. Colloid Interface Sci.*, 2004, **279**, 198–205.
54 I. Greenfeld, C. W. Rodricks, X. Sui and H. D. Wagner, Beaded fiber composites—Stiffness and strength modeling, *J. Mech. Phys. Solids*, 2019, **125**, 384–400.
55 C. E. Marjo, S. Gatenby, A. M. Rich, B. Gong and S. Chee, ATR-FTIR as a tool for assessing potential for chemical ageing in Spandex/LYCRA®/elastane-based fabric collections, *Stud. Conserv.*, 2017, **62**, 343–353.
56 C. Branca, G. D'Angelo, C. Crupi, K. Khouzami, S. Rifici, G. Ruello, *et al.*, Role of the OH and NH vibrational groups in polysaccharide-nanocomposite interactions: A FTIR-ATR study on chitosan and chitosan/clay films, *Polymer*, 2016, **99**, 614–622.

57 E. A. El-Hefian, M. M. Nasef and A. H. Yahaya, The Preparation and Characterization of Chitosan/Poly (Vinyl Alcohol) Blended Films, *J. Chem.*, 2010, **7**, 626235.
58 M. F. Queiroz, K. R. T. Melo, D. A. Sabry, G. L. Sassaki and H. A. O. Rocha, Does the Use of Chitosan Contribute to Oxalate Kidney Stone Formation?, *Mar. Drugs*, 2015, **13**, 141–158.
59 T. Smith, Tensile strength of polyurethane and other elastomeric block copolymers, *J. Polym. Sci. Polym. Phys. Ed.*, 1974, **12**, 1825–1848.
60 C. I. Su, M. C. Maa and H. Y. Yang, Structure and Performance of Elastic Core-Spun Yarn, *Text. Res. J.*, 2004, **74**, 607–610.
61 B. Shi, Z. Hao, Y. Du, M. Jia and S. Xie, Mechanical and barrier properties of chitosan-based composite film as food packaging: A review, *BioResources*, 2024, **19**, 4001–4014.
62 G. Bhat, S. Chand and S. Yakopson, Thermal properties of elastic fibers, *Thermochim. Acta*, 2001, **161**, 367–368.
63 J. Z. Knaul, S. M. Hudson and K. A. M. Creber, Improved mechanical properties of chitosan fibers, *J. Appl. Polym. Sci.*, 1999, **72**, 1721–1732.
64 D. Caschera, A. Mezzi, L. Cerri, T. de Caro, C. Riccucci, G. M. Ingo, *et al.*, Effects of plasma treatments for improving extreme wettability behavior of cotton fabrics, *Cellulose*, 2014, **21**, 741–756.
65 J. Rahmatinejad, A. Khoddami, Z. Mazrouei-Sebdani and O. Avinc, Polyester hydrophobicity enhancement via UV-Ozone irradiation, chemical pre-treatment and fluorocarbon finishing combination, *Prog. Org. Coat.*, 2016, **101**, 51–58.